Supplementary Information for:

Organophosphate Ethyl Paraoxon on Ag and Au Surfaces: A Density Functional Theory Perspective

Hang Hu, Jiří Hostaš, Mohammad Sajjad Ghaemi, Junan Lin, Shiliang Wang, Anguang Hu, and Hsu Kiang Ooi

February 26, 2026

Computational details

All calculations were performed within density functional theory (DFT) using the norm-conserving pseudopotential plane-wave (PP–PW) approach as implemented in CASTEP.[1] The Perdew–Burke–Ernzerhof (PBE) generalized gradient approximation (GGA) was used for the exchange–correlation functional.[2, 3] Norm-conserving pseudopotentials were adopted to represent an effective potential for the core electrons, which do not participate in bonding unlike the valence electrons, while preserving the correct electrostatic potential outside the core region as in all-electron calculations.[4] The reference electron configurations were [Xe] $5d^{10}6s^{0.75}6p^{0.25}$ for Au, [Kr] $5d^{10}5s^{0.75}5p^{0.25}$ for Ag, [Ne] $3s^23p^3$ for P, [He] $2s^22p^4$ for O, [He] $2s^22p^3$ for N, [He] $2s^22p^2$ for C, and $1s^1$ for H. Fractional occupations do not reflect actual atomic physical states and were introduced to improve agreement with experimental IR and Raman spectroscopy results.[5]

The plane-wave kinetic energy cutoff was set to 500 eV. Electronic minimization and geometry optimization were considered converged when the change in total energy fell below 2×10^{-8} eV per atom.

The binding energy was computed as

$$E_{\mathrm{bind}} = E_{\mathrm{slab+mol}} - E_{\mathrm{slab}} - E_{\mathrm{mol}}, \tag{1}$$

where $E_{\mathrm{slab+mol}}$ is the total energy of the relaxed adsorption system, E_{slab} is the energy of the relaxed clean slab, and E_{mol} is the energy of the isolated ethyl paraoxon molecule. All three energies were evaluated with consistent computational settings.

Orbital projected PDOS were obtained from the converged DFT electronic structure by projecting the Kohn–Sham eigenstates onto localized atomic-like basis functions. Optical absorption spectra were computed within linear-response theory by evaluating the frequency-dependent dielectric function, $\varepsilon(\omega) = \varepsilon_1(\omega) + i\varepsilon_2(\omega)$, where $\varepsilon_2(\omega)$ is obtained from interband transitions between occupied and unoccupied Kohn–Sham states within the electric-dipole approximation. Absorption features in the UV–Vis range were derived from $\varepsilon_2(\omega)$ and peak positions were reported consistently across structures. For slab geometries, the optical response can be anisotropic, therefore polarization components were analyzed separately, and in-plane (x–y) absorption was reported. Because periodic slab calculations include vacuum, absolute optical intensities can depend on the supercell volume; consequently, the discussion emphasizes peak positions and relative intensity trends obtained using consistent slab thickness and vacuum spacing across all compared models. Each UV–Vis peak at wavelength λ was converted to excitation energy using $E(\mathrm{eV}) \approx 1240/\lambda(\mathrm{nm})$. For a feature at energy E, the occupied and unoccupied PDOS were inspected in energy windows below and above the Fermi level, with window widths chosen to reflect the applied optical broadening and peak linewidth. The dominant orbital character in these windows was used to qualitatively classify transitions. This PDOS-guided procedure provides an electronic-structure interpretation of adsorption-induced shifts and intensity changes in the UV–Vis spectra.

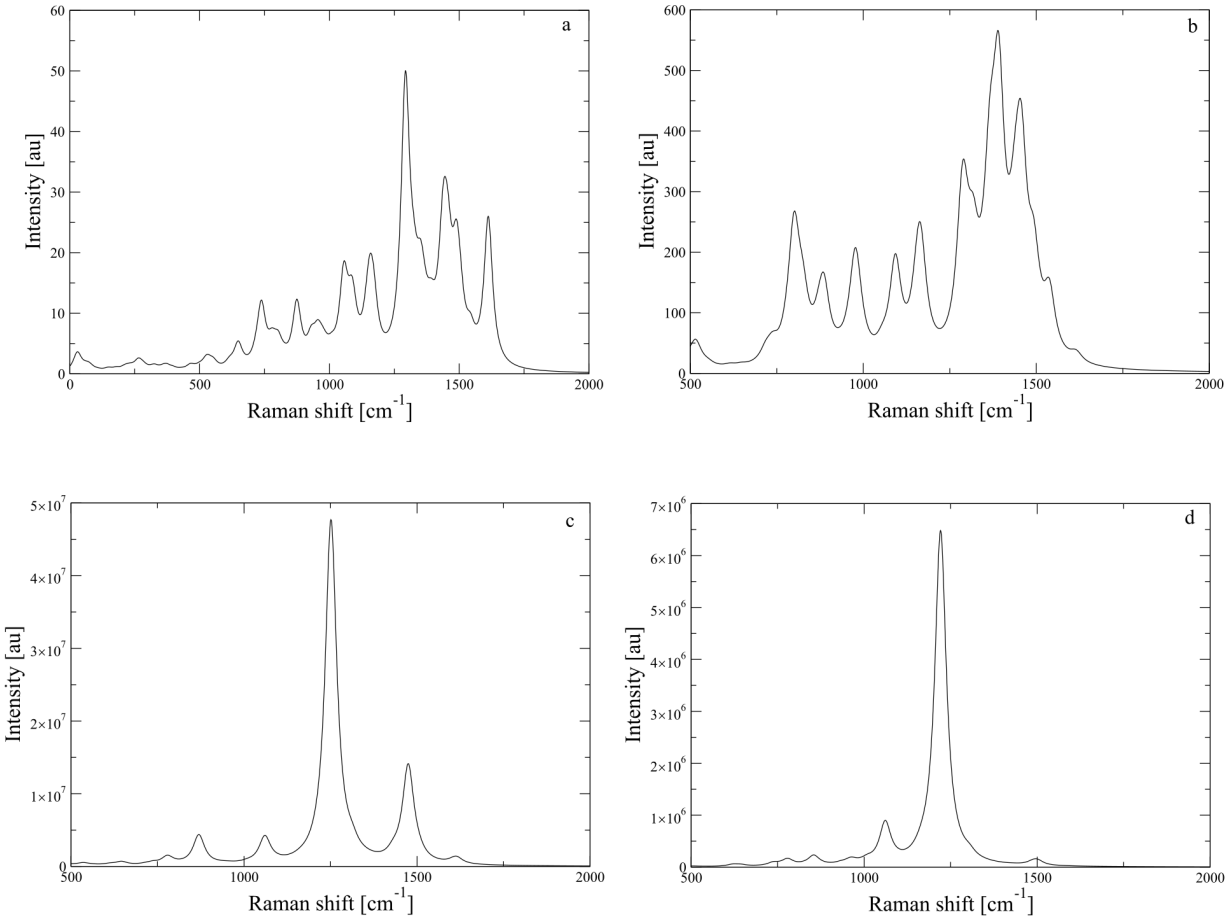

Figure 1: Calculated Raman spectrum of molecular ethyl paraoxon (a), ethyl paraoxon physisorbed on Au (b), ethyl paraoxon-Au complex (c), and ethyl paraoxon-Ag complex (d). The Raman peaks involving the NO_2 moiety and phenyl ring are assigned and labelled. Local regression is adopted to smooth the Raman peaks. Calculated with DFT (PBE/PP-PW).

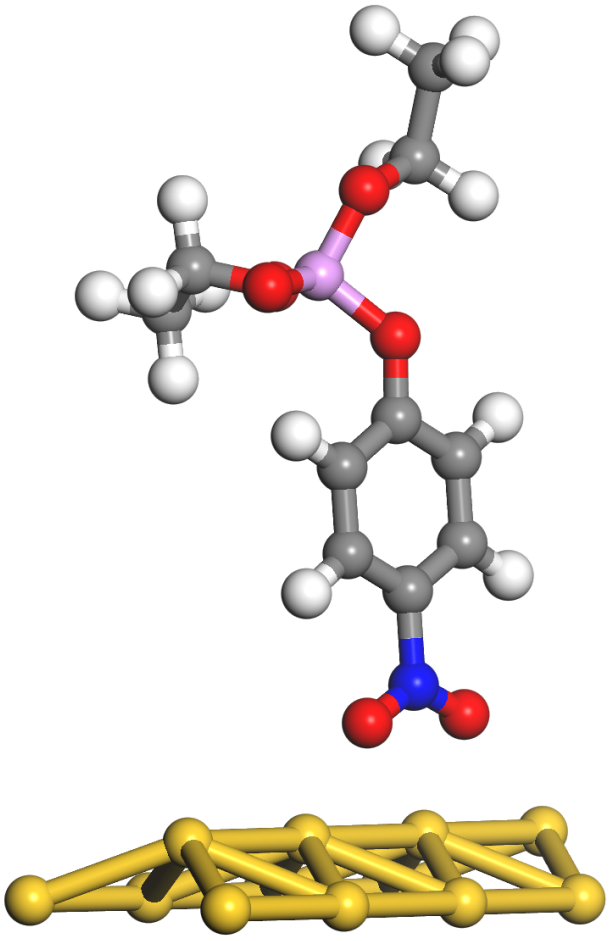

Figure 2: Molecular structure of ethyl paraoxon physisorbed on |110| Au. Grey spheres represent carbon, red spheres oxygen, blue spheres nitrogen, pink spheres phosphorus, white spheres hydrogen and yellow-color spheres gold atoms. The shortest distance between oxygen and gold atoms is 4 Å.

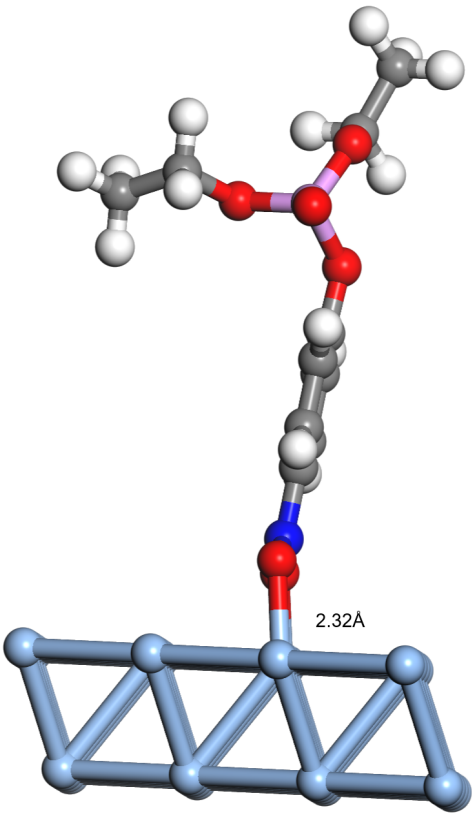

Figure 3: Molecular structure of ethyl paraoxon bonded to an Ag surface. Grey spheres represent carbon, red spheres oxygen, blue spheres nitrogen, pink spheres phosphorus, white spheres hydrogen and grey pearly-color spheres silver atoms. The shortest bond distance between oxygen and silver atoms is shown.

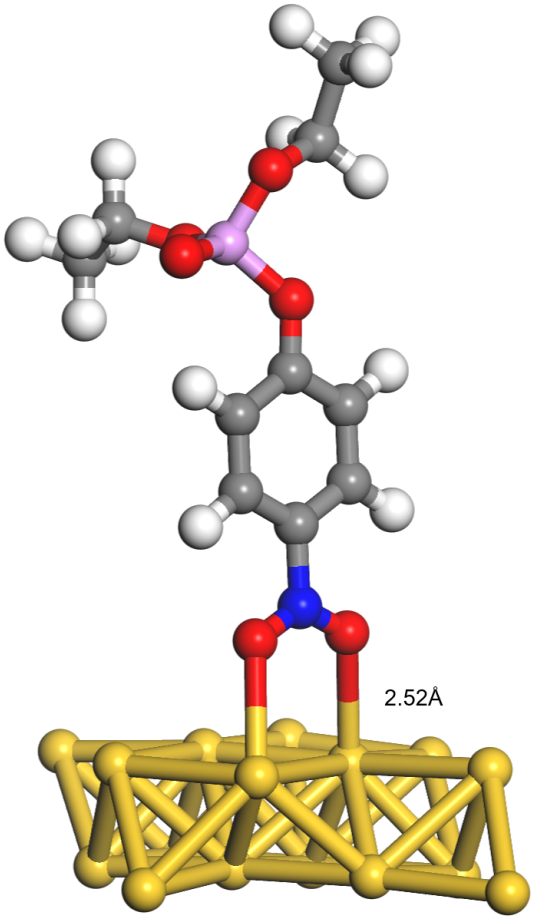

Figure 4: Molecular structure of ethyl paraoxon bonded to an |100| Au surface. Grey spheres represent carbon, red spheres oxygen, blue spheres nitrogen, pink spheres phosphorus, white spheres hydrogen and yellow-color spheres gold atoms. The shortest bond distance between oxygen and gold atoms is shown.

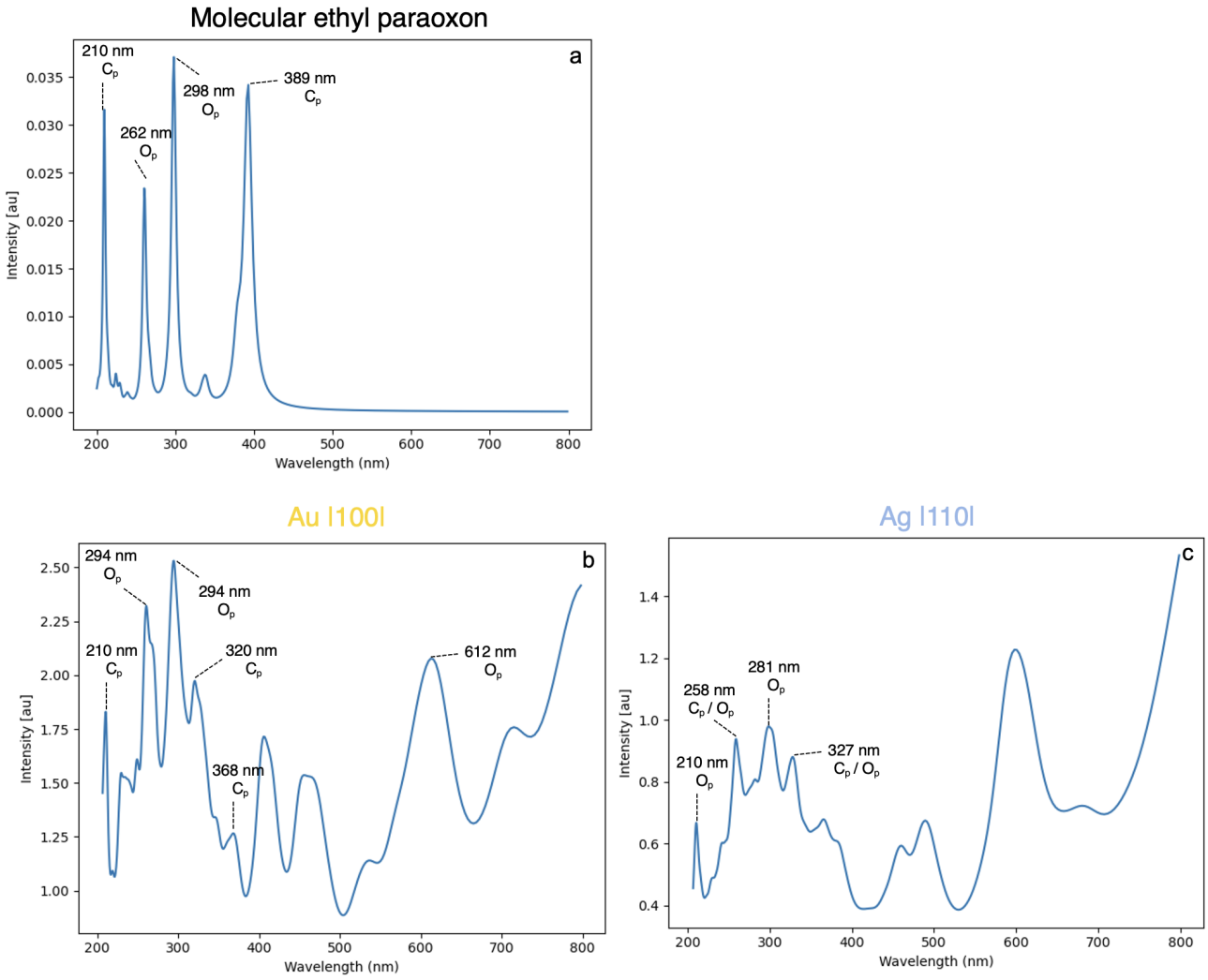

Figure 5: Calculated UV-Vis spectra of molecular ethyl paraoxon (a), ethyl paraoxon-Au complex (b), and ethyl paraoxon-Ag complex (c). PDOS window analysis (Tables S6 and S7) combined with these spectra confirm strong metal–NO_2 coupling in both chemisorbed complexes. Calculated with DFT (PBE/PP-PW).

Table S1: Raman shifts for molecular ethyl paraoxon, physiorbed to Au surface, ethyl paraoxon-Au complex and ethyl paraoxon-Ag complex

	Raman shifts (cm^{-1})[1]				
Mode description	Exp. Molecular[2]	Molecular	Physisorbed on Au	Chemisorbed on Au	Chemisorbed on Ag
NO_2 scissor	857-856	874	871	869	854
C-H bend (in plane)/ NO_2 asymmetric stretch	1110-1145	1095	1093	1099	1097
NO_2 symmetric stretch	1338-1348	1293	1288	1251	1220
NO_2 anti-symmetric stretch	1524-1532	1543	1538	1487	1474
Phenyl ring vibration	1590-1592	1612	1611	1615	1613

[1]Calculated with DFT (PBE/PP-PW). See Computational Methodology section for details.

[2]Experimental reference: F. Fathi, F. Lagugne-Labarthet, D. B. Pedersen and H.-B. Kraatz, *Analyst*, 2012, **137**, 4448–4453. Measured using surface-enhanced Raman spectroscopy.

Table S2. Calculated Molecular ethyl paraoxon phonon frequency at Γ point

Phonon mode	Frequency $[cm^{-1}]^a$
1	0
2	19.27
3	23.54
4	28.68
5	37.37
6	57.96
7	60.63
8	67.95
9	71.18
10	76.06
11	78.38
12	82.77
13	106.75
14	113.26
15	135.89
16	149.11
17	179.29
18	212.37
19	231.63
20	255.92
21	264.54
22	282.31
23	311.9
24	326.59
25	358.31
26	373.28
27	397.47
28	430.41
29	464.73
30	497.37
31	519.58
32	529.36
33	552.14
34	614.85
35	648.45
36	718.34
37	737.91
38	779.04
39	801.48
40	802.49
41	803.16
42	821.22
43	826.45
44	874.36

45	883.71
46	930.14
47	954.97
48	970.25
49	976.16
50	986.1
51	1009.2
52	1055.59
53	1086.54
54	1093.51
55	1095.5
56	1142.72
57	1155.07
58	1161.14
59	1169.88
60	1170.59
61	1284.94
62	1289.87
63	1293.02
64	1296.51
65	1324.53
66	1351.26
67	1359.15
68	1363.62
69	1366.25
70	1386.86
71	1394.53
72	1430.8
73	1440.01
74	1440.37
75	1455.9
76	1456.68
77	1486.57
78	1490.22
79	1503.72
80	1543.57
81	1612.3
82	1619.42
83	3007.88
84	3011.54
85	3040.96
86	3044.55
87	3049.04
88	3062.88
89	3128.59
90	3130.29
91	3132.02
92	3134.32

93	3189.78
94	3191.87
95	3206.82
96	3208.49

Selected phonon frequency calculated with DFT (PBE/FP-NAO)

Table S3. Calculated ethyl paraoxon physisorbed on an Au surface phonon frequency at point

Phonon mode	Frequency [cm^{-1}][a]
1	0
2	0
3	0
4	0
5	0
6	0
7	0
8	5.43
9	8.46
10	17.15
11	18.11
12	26.19
13	28.31
14	29.95
15	31.58
16	32.66
17	33.93
18	35.19
19	38.91
20	40.44
21	43.57
22	47.25
23	51.31
24	54.75
25	55.54
26	57.68
27	58.25
28	61.21
29	62.5
30	64.37
31	65.22
32	66.75
33	67.46
34	70.94
35	73.15
36	73.53

37	77.35
38	78.18
39	82.87
40	88.25
41	92.25
42	93.36
43	94.87
44	97.28
45	97.87
46	106.09
47	108.54
48	109.73
49	110.52
50	116.17
51	117.37
52	119.47
53	120.25
54	123.28
55	128.66
56	129.51
57	131.88
58	133.72
59	135.33
60	136.82
61	138.37
62	147.05
63	148
64	152.97
65	163.92
66	224.94
67	234.03
68	260.05
69	264.51
70	282.37
71	313.02
72	322.37
73	351.01
74	380.53
75	415.4
76	428.64
77	455.46
78	504.37
79	509.85
80	537.23
81	557.62
82	619.6
83	643.62
84	705.86

85	737.33
86	768.4
87	779.05
88	801.87
89	803.53
90	818.97
91	823.98
92	854.19
93	873.63
94	932.67
95	960.84
96	969.86
97	972.46
98	983.65
99	1008.27
100	1060.89
101	1086.28
102	1091.57
103	1097.09
104	1149.92
105	1156.57
106	1161.87
107	1167.19
108	1168.81
109	1220.84
110	1285.32
111	1290.58
112	1291.59
113	1304.61
114	1345.73
115	1351.64
116	1362.89
117	1364.85
118	1388.49
119	1390.84
120	1428.89
121	1440.05
122	1440.74
123	1455.1
124	1456.26
125	1486.97
126	1487.44
127	1490.85
128	1501.71
129	1598.98
130	1613.3
131	3004.41
132	3009.08

133	3037.32
134	3046.54
135	3053.16
136	3059.78
137	3123.91
138	3127.87
139	3132.67
140	3139.54
141	3183.3
142	3191.93
143	3213.13
144	3217.67

Selected phonon frequency calculated with DFT (PBE/FP-NAO)

Table S4. Calculated ethyl paraoxon-Au complex phonon frequency at point

Phonon mode	Frequency [cm^{-1}][a]
1	0
2	0
3	0
4	0
5	0
6	0
7	0
8	21.35
9	24.76
10	25.62
11	26.86
12	30.1
13	34.17
14	35.2
15	35.63
16	36.48
17	38.17
18	41.74
19	43.3
20	43.38
21	48.18
22	49.94
23	51.31
24	52.83
25	52.95
26	54.24
27	54.35
28	56.32
29	57.26

30	57.7
31	58.41
32	62.71
33	63.66
34	64.24
35	65.41
36	66.33
37	71.08
38	71.6
39	74.68
40	75.02
41	76.32
42	78.09
43	79.57
44	83.22
45	85.34
46	86.94
47	90.75
48	94.27
49	96.74
50	98.39
51	100.68
52	103.28
53	105.06
54	105.83
55	107.78
56	108.87
57	111.09
58	113.6
59	118.26
60	119.63
61	121.02
62	126.95
63	147.71
64	156.5
65	172.18
66	226.75
67	235.24
68	256.31
69	268.57
70	284.78
71	315.13
72	318.9
73	353.37
74	372.78
75	403.57
76	427.96
77	460.4

78	498.36
79	516.65
80	535.13
81	556.5
82	612.56
83	645.68
84	715.9
85	736.69
86	777.57
87	789.75
88	800.58
89	801.82
90	820.52
91	824.37
92	869.25
93	879.7
94	930
95	954.68
96	968.35
97	974.71
98	988.97
99	1010.08
100	1060.12
101	1082.22
102	1091.94
103	1099.82
104	1134.36
105	1157.33
106	1161.37
107	1166.98
108	1169.48
109	1251.22
110	1287.94
111	1291.37
112	1294.33
113	1313.02
114	1341.65
115	1356.01
116	1368.87
117	1370.91
118	1387.54
119	1392.71
120	1430.73
121	1439
122	1440.44
123	1455.14
124	1456.46
125	1474.39

126	1488.18
127	1491.78
128	1504.87
129	1604.66
130	1615.51
131	3008.77
132	3009.81
133	3044.12
134	3047.3
135	3051.02
136	3054.52
137	3130.7
138	3133.85
139	3134.19
140	3136.18
141	3191.01
142	3194.06
143	3208.65
144	3210.01

Selected phonon frequency calculated with DFT (PBE/FP-NAO)

Table S5. Calculated ethyl paraoxon-Ag complex phonon frequency at point

Phonon mode	Frequency [cm^{-1}][a]
1	0
2	0
3	0
4	0
5	0
6	0
7	0
8	5.43
9	8.46
10	17.15
11	18.11
12	26.19
13	28.31
14	29.95
15	31.58
16	32.66
17	33.93
18	35.19
19	38.91
20	40.44
21	43.57
22	47.25

23	51.31
24	54.75
25	55.54
26	57.68
27	58.25
28	61.21
29	62.5
30	64.37
31	65.22
32	66.75
33	67.46
34	70.94
35	73.15
36	73.53
37	77.35
38	78.18
39	82.87
40	88.25
41	92.25
42	93.36
43	94.87
44	97.28
45	97.87
46	106.09
47	108.54
48	109.73
49	110.52
50	116.17
51	117.37
52	119.47
53	120.25
54	123.28
55	128.66
56	129.51
57	131.88
58	133.72
59	135.33
60	136.82
61	138.37
62	147.05
63	148
64	152.97
65	163.92
66	224.94
67	234.03
68	260.05
69	264.51
70	282.37

71	313.02
72	322.37
73	351.01
74	380.53
75	415.4
76	428.64
77	455.46
78	504.37
79	509.85
80	537.23
81	557.62
82	619.6
83	643.62
84	705.86
85	737.33
86	768.4
87	779.05
88	801.87
89	803.53
90	818.97
91	823.98
92	854.19
93	873.63
94	932.67
95	960.84
96	969.86
97	972.46
98	983.65
99	1008.27
100	1060.89
101	1086.28
102	1091.57
103	1097.09
104	1149.92
105	1156.57
106	1161.87
107	1167.19
108	1168.81
109	1220.84
110	1285.32
111	1290.58
112	1291.59
113	1304.61
114	1345.73
115	1351.64
116	1362.89
117	1364.85
118	1388.49

119	1390.84
120	1428.89
121	1440.05
122	1440.74
123	1455.1
124	1456.26
125	1486.97
126	1487.44
127	1490.85
128	1501.71
129	1598.98
130	1613.3
131	3004.41
132	3009.08
133	3037.32
134	3046.54
135	3053.16
136	3059.78
137	3123.91
138	3127.87
139	3132.67
140	3139.54
141	3183.3
142	3191.93
143	3213.13
144	3217.67

Table S6: Au complex: PDOS-window composition for representative UV–Vis peaks. Occupied and unoccupied contributions are normalized within the selected energy window for each peak.

Peak	Occupied-side	Unoccupied-side
210 nm	Au *d* 77%, O(*p*) 16%	Au *s* 47%, C(*p*) 44%
260 nm	Au *d* 87%, C(*p*) 5%, O(*p*) 5%	C(*p*) 46%, Au *s* 45%
294 nm	Au *d* 78%, O(*p*) 15%	Au *s* 44%, O(*p*) 20%, N(*p*) 11%, C(*p*) 12%
320 nm	Au *d* 61% (mixed)	Au *d* 77%, Au *s* 22%
368 nm	Au *d* 73% (mixed)	Au *d* 77%, Au *s* 22%
612 nm	Au *d* 79%, O(*p*) 15%	Au *d* 77%, Au *s* 22%

Table S7: Ag complex: PDOS-window composition for representative UV–Vis peaks. Occupied and unoccupied contributions are normalized within the selected energy window for each peak.

Peak	Occupied-side	Unoccupied-side
210 nm	Ag d 82%, O(p) 13%	C(p) 77%, Ag s 19%
258 nm	Ag d 75%, C(p) 9%, O(p) 9%	C(p) 77%, Ag s 19%
281 nm	Ag d 82%, O(p) 13%	Ag s 90%, Ag d 7%
327 nm	Ag d 75%, C(p) 9%, O(p) 8%	Ag s 89%, Ag d 8%
365 nm	Ag s 79%, Ag d 19%	C(p) 77%, Ag s 19%
489 nm	Ag s 86%, Ag d 12%	C(p) 77%, Ag s 20%
597 nm	Ag s 82%, Ag d 11%, O(p) 3%, N(p) 2%	C(p) 77%, Ag s 20%

Sample Castep simulation input parameters

task : GeometryOptimization
- comment : CASTEP calculation from Materials Studio
- xc_functional : PBE
- spin_polarized : false
- opt_strategy : Default
- page_wvfns : 0
- cut_off_energy : 489.800000000000010
- grid_scale : 1.500000000000000
- fine_grid_scale : 1.500000000000000
- finite_basis_corr : 0
- elec_energy_tol : 2.000000000000000e-006
- max_scf_cycles : 100
- fix_occupancy : false
- metals_method : dm
- mixing_scheme : Pulay
- mix_charge_amp : 0.500000000000000
- mix_charge_gmax : 1.500000000000000
- mix_history_length : 20
- nextra_bands : 85
- smearing_width : 0.100000000000000
- num_dump_cycles : 0
- geom_energy_tol : 2.000000000000000e-005
- geom_force_tol : 0.050000000000000
- geom_stress_tol : 0.100000000000000
- geom_disp_tol : 0.002000000000000
- geom_max_iter : 100
- geom_method : BFGS
- fixed_npw : false
- calculate_ELF : false
- calculate_stress : false
- popn_calculate : true
- calculate_hirshfeld : true
- calculate_densdiff : false
- popn_bond_cutoff : 3.000000000000000
- pdos_calculate_weights : false

Appendix: XYZ Structures

ethyl paraoxon-Ag-complex

```
64
Ag 9.035794 2.433546 2.415834
Ag -4.518469 8.520385 0.043110
Ag -1.506919 8.520385 0.043110
Ag 3.010406 0.696148 0.043110
Ag 6.021956 0.696148 0.043110
Ag -1.504631 10.257783 2.415834
Ag 1.506919 10.257783 2.415834
Ag 6.024244 2.433546 2.415834
Ag -0.001144 0.696148 0.043110
Ag 4.518469 10.257783 2.415834
Ag -4.516181 10.257783 2.415834
Ag 0.001144 2.433546 2.415834
Ag 3.012694 2.433546 2.415834
Ag 1.504631 8.520385 0.043110
Ag 4.516181 8.520385 0.043110
Ag 9.033506 0.696148 0.043110
Ag -3.012694 5.912306 0.043110
Ag 7.530019 5.041625 2.415834
Ag -1.504631 5.041625 2.415834
Ag -3.010406 7.649704 2.415834
Ag 0.001144 7.649704 2.415834
Ag 4.516181 3.304227 0.043110
Ag 7.527731 3.304227 0.043110
Ag 6.021956 5.912306 0.043110
Ag 6.024244 7.649704 2.415834
Ag -1.506919 3.304227 0.043110
Ag 1.504631 3.304227 0.043110
Ag -0.001144 5.912306 0.043110
Ag 3.010406 5.912306 0.043110
Ag 1.506919 5.041625 2.415834
Ag 4.518469 5.041625 2.415834
Ag 3.012694 7.649704 2.415834
P 0.519432 6.562761 11.599738
O 0.341992 5.501586 10.376718
O 2.113446 6.746683 11.586832
O 0.162925 5.634806 12.837585
O -0.270618 7.801181 11.533836
O 0.301577 7.505529 4.425002
O 1.357306 5.622496 4.205331
N 0.784569 6.473669 4.873406
C 0.459382 5.805479 9.032605
C 2.737499 7.961734 12.098117
C 0.792941 4.349337 13.093776
```

C -0.092214 6.964301 8.483153
C 1.106564 4.862293 8.233551
C 0.669588 6.239046 6.324883
C 0.019997 7.181814 7.115974
C 1.212691 5.078034 6.867471
C 4.174490 7.974253 11.626922
C 0.299950 3.856201 14.435967
H 2.176568 8.821670 11.730442
H 2.672148 7.947233 13.189608
H 0.515397 3.669984 12.285661
H 1.877822 4.483287 13.082518
H -0.600142 7.674637 9.121847
H 1.518785 3.972626 8.693762
H -0.394573 8.068248 6.655488
H 1.709476 4.367593 6.220265
H 4.678684 8.870493 11.996793
H 4.717412 7.100234 11.993498
H 4.224181 7.977904 10.535431
H 0.742648 2.882240 14.659758
H 0.574784 4.550472 15.232276
H -0.785894 3.748331 14.433222

ethyl paraoxon-Au-complex

48
Au 0.000000 2.495040 2.079198
Au 0.000000 4.574240 0.000000
Au 2.079200 2.495040 0.000000
Au 2.079200 4.574240 2.079198
Au 4.158400 2.495040 2.079198
Au 4.158400 4.574240 0.000000
Au 6.237600 2.495040 0.000000
Au 6.237600 4.574240 2.079198
Au 0.000000 6.653440 2.079198
Au 0.000000 0.415840 0.000000
Au 2.079200 6.653440 0.000000
Au 2.079200 0.415840 2.079198
Au 4.158400 6.653440 2.079198
Au 4.158400 0.415840 0.000000
Au 6.237600 6.653440 0.000000
Au 6.237600 0.415840 2.079198
P 3.346015 4.992741 11.197908
O 3.244467 3.701808 10.209643
O 4.902587 5.349199 11.040042
O 3.165624 4.287726 12.608769
O 2.406383 6.097795 10.957024
O 2.678010 4.498141 4.006050
O 3.947652 2.739554 4.068534

```
N 3.305678 3.633776 4.604396
C 3.260518 3.750960 8.827485
C 5.394360 6.702675 11.270990
C 3.961209 3.155560 13.055873
C 2.544359 4.711800 8.111236
C 3.981502 2.750116 8.175486
C 3.288546 3.673115 6.078625
C 2.564901 4.671796 6.723116
C 3.996222 2.707950 6.789133
C 6.795158 6.785677 10.706866
C 3.596517 2.879193 14.497424
H 4.714628 7.406360 10.789222
H 5.382383 6.892465 12.347793
H 3.732663 2.305750 12.410056
H 5.019521 3.406229 12.944373
H 1.982808 5.470458 8.640033
H 4.521927 2.018571 8.763897
H 2.022479 5.399849 6.135368
H 4.546462 1.946214 6.252829
H 7.201018 7.787685 10.866941
H 7.458756 6.066108 11.191505
H 6.792996 6.583579 9.633155
H 4.166550 2.023228 14.867692
H 3.819989 3.740897 15.129109
H 2.533464 2.651063 14.590377
```

ethyl paraoxon physisorbedon Au

```
48
Au 1.763162 9.672904 1.470279
Au 3.842362 5.262229 0.000000
Au 3.842362 8.202679 0.000000
Au 1.763162 6.732454 1.470279
Au 3.842362 11.143129 0.000000
Au 3.842362 2.321779 0.000000
Au 1.763162 0.851554 1.470279
Au 1.763162 3.792004 1.470279
Au 5.921562 9.672904 1.470279
Au 8.000762 5.262229 0.000000
Au 8.000762 8.202679 0.000000
Au 5.921562 6.732454 1.470279
Au 8.000762 11.143129 0.000000
Au 8.000762 2.321779 0.000000
Au 5.921562 0.851554 1.470279
Au 5.921562 3.792004 1.470279
P 2.975169 6.311735 10.505369
O 2.026056 5.365968 9.578930
O 4.390938 5.586620 10.294102
```

```
O 2.453123 5.912657 11.950528
O 2.947640 7.757378 10.237850
O 1.805993 6.221404 3.361160
O 1.661281 4.059115 3.472161
N 1.764575 5.167194 3.982722
C 2.004432 5.367027 8.196034
C 5.643864 6.316322 10.452123
C 2.362553 4.542290 12.428884
C 2.033957 6.549794 7.454668
C 1.888329 4.124275 7.572325
C 1.846246 5.236589 5.453431
C 1.958523 6.479340 6.069626
C 1.807074 4.055939 6.189429
C 6.746172 5.473001 9.851172
C 1.974076 4.590866 13.889716
H 5.548220 7.282671 9.955732
H 5.806790 6.490396 11.519192
H 1.613792 4.023241 11.827504
H 3.330213 4.055586 12.280525
H 2.112051 7.502029 7.962224
H 1.864211 3.227791 8.179931
H 1.978983 7.374413 5.463092
H 1.718085 3.108409 5.675003
H 7.705349 5.986168 9.956161
H 6.819360 4.504887 10.351428
H 6.564783 5.298573 8.788182
H 1.882924 3.575705 14.284339
H 2.725914 5.122029 14.476497
H 1.016313 5.097564 14.018323
```

References

[1] Stewart J. Clark, Matthew D. Segall, Chris J. Pickard, Phil J. Hasnip, Matt I. J. Probert, Keith Refson, and Mike C. Payne. First principles methods using castep. *Zeitschrift für Kristallographie - Crystalline Materials*, 220(5-6):567–570, 5 2005. ISSN 2196-7105. doi: 10.1524/zkri.220.5.567.65075.

[2] John P. Perdew, Kieron Burke, and Matthias Ernzerhof. Generalized gradient approximation made simple. *Physical Review Letters*, 77(18):3865–3868, 10 1996. doi: 10.1103/PhysRevLett.77.3865.

[3] Daniel Sanchez-Portal, Emilio Artacho, and Jose M Soler. Projection of plane-wave calculations into atomic orbitals. *Solid State Communications*, 95(10):685–690, 9 1995. ISSN 0038-1098. doi: 10.1016/0038-1098(95)00341-X.

[4] D. R. Hamann, M. Schlüter, and C. Chiang. Norm-conserving pseudopotentials. *Physical Review Letters*, 43(20):1494–1497, 11 1979. doi: 10.1103/PhysRevLett.43.1494.

[5] Shizhuang Weng, Miao Li, Cheng Chen, Xiang Gao, Shouguo Zheng, and Xinhua Zeng. Fast and

accurate determination of organophosphate pesticides using surface-enhanced raman scattering and chemometrics. *Analytical Methods*, 7(6):2563–2567, 3 2015. ISSN 1759-9679. doi: 10.1039/C4AY03067B.